Drug Delivery and Translational Research (2019) 9:227–239
https://doi.org/10.1007/s13346-018-00609-8

ORIGINAL ARTICLE

pH-responsive calcium alginate hydrogel laden with protamine nanoparticles and hyaluronan oligosaccharide promotes diabetic wound healing by enhancing angiogenesis and antibacterial activity

Tao Wang[1] · Yan Zheng[1] · Yijie Shi[1] · Liang Zhao[1]

Published online: 5 December 2018

Abstract
Diabetic wounds as chronic wounds represent a severe, persistent complication of diabetes and, in the most extreme cases, can lead to amputation. Two critical and unfavorable factors affecting diabetic wound healing are sustained bacterial-induced chronic inflammation and disrupted vascularization. In this paper, we presented a novel, pH-responsive calcium alginate hydrogel laden with protamine nanoparticles and hyaluronan oligosaccharides, and explored its potential for accelerating diabetic wound healing. A thorough investigation indicated that the drug- and nanoparticle-loaded hydrogel demonstrated strong bactericidal behavior mediated by protamine nanoparticles and reduced bacterial-induced chronic inflammation at the wound site. Furthermore, it accelerated the wound-healing process by promoting angiogenesis in skin wounds with the hyaluronan oligosaccharide-mediated enhanced expression of vascular endothelial growth factor.

Keywords Diabetes · Bacterial · Inflammation · Calcium alginate hydrogel · Protamine · Nanoparticles

Introduction

Wound-healing impairment in diabetic patients represents a particularly challenging clinical problem in which there is currently no efficacious treatment [1, 2]. It was thought that impaired angiogenesis and bacteria-induced inflammation are major contributors that delay diabetic wound healing [3–7]. It was found that bacteria were by far the most frequently isolated microorganisms; they invaded from the ulcer's surface to the deep tissues. Compared with non-diabetic patients, diabetic ulcer wound sites are associated with alkaline pH levels, which contributes to the increased incidence of various bacterial infections in these patients [8, 9]. Bacterial infections caused varying degrees of cell degeneration, necrosis, and tissue defects, thus enhancing local inflammation [10, 11]. Wound infection caused by excessive local inflammation showed a negative impact on wound repair, thus extending the wound-healing time. In addition, it was reported that *Escherichia coli* bacillus may reduce the contents of protein, oxyproline, collagen type I, and collagen type III in the wound, consequently delaying the restoration of infectious wounds [12, 13]. The number of positive cells for integrin β1 and K19 that acted on promoting wound epithelialization in bacteria-infected wounds was less than that in non-infected wounds, thus prolonging the wound-healing effects [14]. Therefore, it was necessary to prevent and control the further proliferation of bacteria at the diabetic wound site.

Ineffective vascular repair is likely to be another important contributor to diabetic vascular disease, and this effect is linked with impaired neovascularization in diabetes [15–17]. Vascular endothelial growth factor (VEGF), originally known as vascular permeability factor (VPF), is a signal protein produced by cells that stimulate the formation of blood vessels. It was found that when compared with healthy mice, the expression of VEGF was significantly reduced during wound healing in diabetic mice. This indicated that wound healing in genetically diabetic mice was impaired and that inadequate VEGF expression prolonged angiogenesis, reduced capillary density, and significantly decreased

Tao Wang and Yan Zheng contributed equally to this work.

✉ Liang Zhao
liangzhao79@163.com

[1] School of Pharmacy, Jinzhou Medical University, Jinzhou 121000, People's Republic of China

blood flow in the wound [18]. Small fragments, or hyaluronan oligosaccharides (HAOs), stimulated endothelial cell proliferation, motility, and tubule formation, and induced angiogenesis in a variety of experimental systems [19–21]. It was reported that the co-addition of HAO and VEGF induced an in vitro angiogenic response that was greater than the sum of the effects elicited by either agent separately [22]. This indicated that HAO had the ability to promote new blood vessel formation in vivo and suggested that hyaluronate metabolism plays a pivotal role in the regulation of angiogenesis through the mediation of VEGF.

As hydrogel dressings act as absorbents for wound exudate and are made up of three-dimensional networks for loading more therapeutic drugs, it has attracted much attention for wound healing application in recent years [23, 24]. Based on the hypothesis on regulating antibacterial and neovascularization activities for promoting diabetic wound healing, we prepared a novel pH response Ca-alginate (CaAlg) hydrogel loaded with protamine nanoparticles (NPs) and HAO (protamine NPs/HAO Ca-alginate hydrogel). Clinical studies indicated that a pH level at the diabetic wound site becomes more alkaline, accelerating bacterial colonialization and biofilm formation, thus prolonging the inflammatory phase and impairing the formation of blood vessels. Therefore, we used CaAlg as pH-sensitive dressing material to trigger more rapid and complete drug release, owing to its increased swelling and hydration disruption in alkaline wound fluid in diabetic ulcers (Fig. 1). Since protamine, as a cationic antimicrobial peptide (CAP), was active against a variety of bacteria by causing general disruptions to the cell envelope of bacteria [25, 26], we investigated the enhanced antibacterial effects of protamine NPs loaded in hydrogel against both Gram-positive and Gram-negative bacteria. In addition, human umbilical vein endothelial cells (HUVECs) were treated with a specific HAO-loaded hydrogel, and it was determined whether HAO was able to trigger neovascularization by stimulating the secretion of VEGF. We further evaluated the in vivo effectiveness of the hydrogel composite at accelerating wound healing in a diabetic mouse-skin defect model.

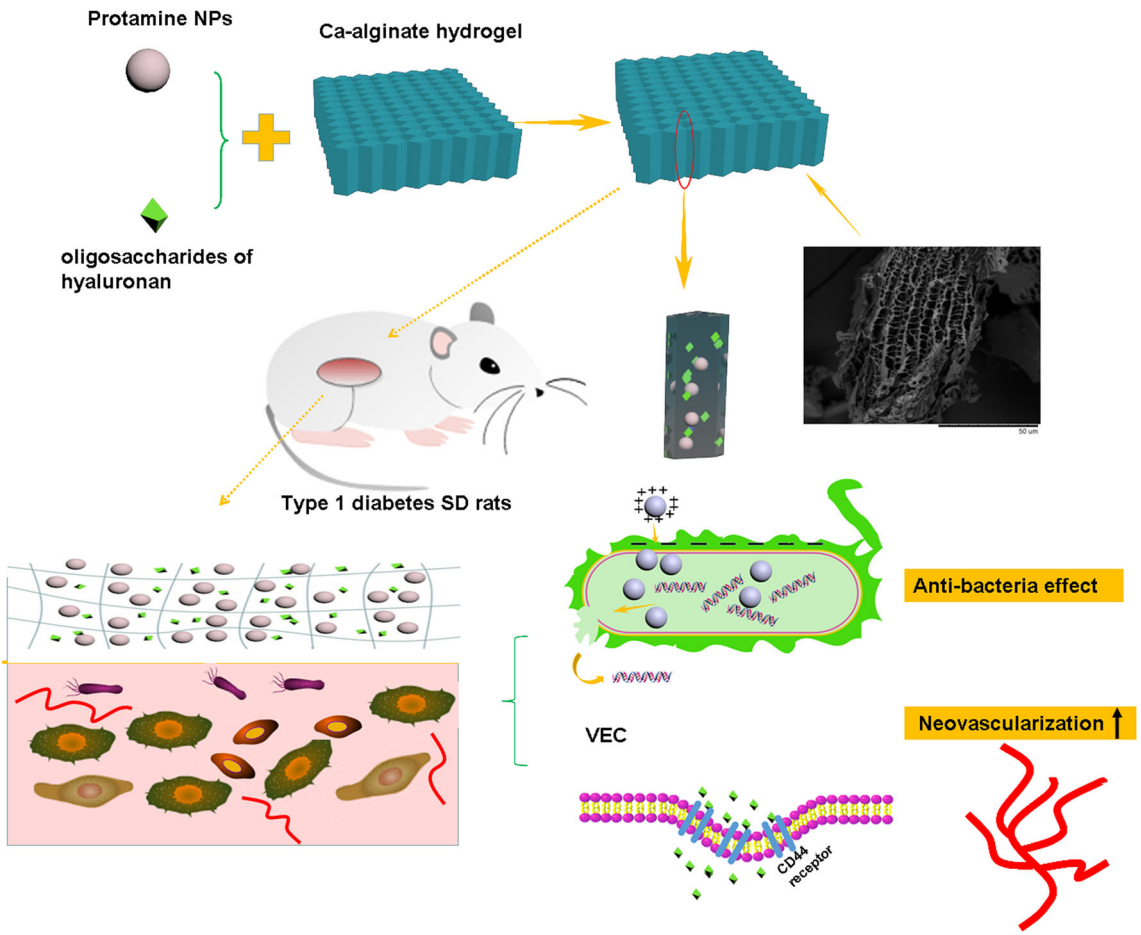

Fig. 1 The primary hypothesis of this study. Protamine NPs and HAO were loaded into the pores of Ca-alginate hydrogel and showed complete and fast release at the alkaline diabetic wound sit. Protamine NPs/HAO Ca-alginate hydrogel was placed on the wound in streptozotocin-induced type 1 diabetic rats, and protamine NPs exhibited antibacterial activity by damaging the cell wall, thus reducing inflammatory response. Moreover, HAO significantly enhanced HUVEC migration and capillary-like tube formation with HAO-induced the stimulation of VEGF, and led to rapid diabetic wound healing

Materials and methods

Sodium alginate with a molecular weight of approximately 160 kDa was purchased from Qingdao Huanghai Biological Pharmaceutical Co., Ltd. (Qingdao, People's Republic of China), and protamine was purchased from Tianjin Sixth Pharmaceutical Co., Ltd. (Tianjin, People's Republic of China). Purified HAO with molecular weights <1 0 kDa were obtained from Sigma-Aldrich Co. (St. Louis, MO, USA). HUVECs were obtained from the Cell Line Bank of the Chinese Academy of Sciences (Shanghai, People's Republic of China). Cells were cultured in standard medium with complete F-12K growth medium (Gibco), 0.1 mg/ml heparin, 0.03 mg/ml endothelial cell growth supplement (ECGS) (Sigma-Aldrich), FBS 10%, gentamicin 3%, and amphotricin D 3% (Gibco) at 37 °C in a 5% CO_2 environment. Human foreskin fibroblasts (HFFs; Cell Bank of the Chinese Academy of Sciences, Shanghai, China) were cultured in high-glucose Dulbecco's modified eagle medium (Gibco BRL) with 10% FBS. Cells that had grown to 80% confluence were used in the experiments. Other chemicals purchased were of analytical grade and were obtained from Sigma-Aldrich Co.

The preparation and characterization of pH-responsive protamine NPs/HAO Ca-alginate hydrogel

According to our previous reports [27–29], the preparation of protamine NPs was typically described as follows: certain amount of protamine was swelled with distilled water overnight to obtain an aqueous solution containing protamine at 4 mg/mL followed by the addition of 1 mL of ethanol at 37 °C under continuous stirring (1000 rpm). The resulting white suspension was further stirred for 24 h, and then ethanol was removed with vacuum distillation succeeded by the addition of 8% glutaraldehyde in water (0.5 μL per mg of protamine) for particle cross-linking. After washing with cold PBS three times, the protamine NPs were collected to determine their hydrodynamic diameter, polydispersity, zeta potential, and morphology. To obtain the pH-responsive drug- and NP-loaded hydrogels, the obtained protamine NPs and HAO were dispersed in 100 mL of 0.1 M $CaCl_2$ solution followed by the quick addition of 20 mL of 1% (*w*/*v*) freshly prepared sodium alginate solution; moreover, Ca-alginate hydrogel with a gelling and porous network was formed owing to the replacement of Na^+ ions of Na-alginate with Ca^{2+} ions. Scanning electron microscopy (S-4800, Hitachi, Japan) was used to observe the morphology of the hydrogel. The encapsulated efficiency and loading rate of HAO in CaAlg hydrogel were measured with a UV-Vis spectrometer using a previously reported method [30].

Rheological properties, swelling ratio, and drug release of protamine NPs/HAO CaAlg hydrogel in vitro

The rheological properties of the protamine NPs/HAO CaAlg hydrogel were assessed using a rotational rheometer (Anton Paar MCR302) to determine the elastic modulus (G′), viscous modulus (G″), and phase angle (δ) at the linear viscoelastic region. The swelling capacity of the gels was also determined by calculating the difference between the initial weight of the gel (W_0) and the weight of the absorbent gel (W_S), as follows: swelling ratio (SR) (%) = 100 × (Ws–W_0)/W_0. The appropriate amount of protamine NPs/HAO-loaded CaAlg hydrogel was encapsulated in a dialysis bag (molecular weight [Mw] 3000–4000) and placed in 20 mL of phosphate-buffered saline (PBS) with different pH levels. At predetermined time points, the incubation media was removed and the amount of released HAO was assayed by detecting its absorbance with ultraviolet-visible spectrophotometry.

MTT assay and hemolysis analysis

According to our previous reports [31], cell viability was assessed via MTT assay. The extracts of protamine NP/HAO CaAlg hydrogel were co-incubated with HFF cells and HUVECs, which were seeded into a 96-well plate at 1000–100,000 per well. Following that, an MTT solution was added and dimethyl sulfoxide (DMSO) was used to dissolve the formazan deposit. Finally, the absorbance was measured at 490 nm. In terms of hemolysis analysis, the extracts of protamine NP/HAO CaAlg hydrogel were also added into the erythrocyte suspension, respectively, for continuous incubation at 37 °C. Saline solution and 0.3% Triton were used as negative and positive control groups, and hemolysis of blood samples treated with hydrogel was analyzed by observing the color change of the serum and plasma.

Antibacterial activities of protamine NPs/HAO-loaded CaAlg hydrogel

To evaluate the antibacterial activities of protamine NP/HAO CaAlg hydrogel, 100 μL of protamine NPs/HAO CaAlg hydrogel and HAO-loaded CaAlg hydrogel was placed into a tube respectively and incubated with 5 mL of bacterial suspension containing 1×10^6 CFU of *Escherichia coli* and *Staphylococcus aureus* for continuous shaking for 24 h at 37 °C. Sterilized cotton swab was used to dip into bacteria suspension treated with both gels and slowly scratched on the LB-agar growth plates for incubation at 37 °C. After subculture of the bacteria on agar plates for 24 h, all the plates were imaged. In order to determine the concentration of bacterial, 100 μL of bacteria suspension treated with different formulations was pipetted to 96-well plates after the bacteria solution showed slight turbidity. The optical density (OD) of the

bacteria suspension was measured on a microplate reader at 600 nm. In addition, the OD at 260 nm was also evaluated to assess for leakage of DNA and RNA from the bacteria.

Capillary-like tube formation assay

Matrigel (150 μL/well) was added to a 24-well plate and polymerized for 30 min at 37 °C. Extracts of the protamine NPs/HAO CaAlg hydrogel were co-incubated with HUVECs (80 μL/well, about 1×10^5 cells/well) and placed in the bottom of Matrigel-loaded 24-well plates for 24 h. The formation of HUVECs into capillary-like structures on Matrigel (BD Biosciences, Bedford, MA, USA) was evaluated by counting the number of connected cells using a confocal microscope (TCS SP8; Leica Microsystems, Wetzlar, Germany) and imaged at × 100 magnification. The migration of HUVECs was detected using the transwell method. The extract of the protamine NP/HAO-loaded CaAlg hydrogel was placed into the transwell insert pre-coated with basement membrane Matrigel and incubated with HUVECs for 24 h in an incubator set at 37 °C, 5% CO_2. Migration was determined by counting cells on the lower surface of the filter and the cell migration rate was calculated using the following formula: relative rate of migration [%] = migrating cells with treatment/migrating cells without treatment × 100.

Western blot assay

After treatment with the extract of hydrogels, HUVECs were collected, washed twice with ice-cold PBS, then lysed in radioimmunoprecipitation assay buffer (1% Nonidet P 40, 1% phenylmethanesulfonyl fluoride, 150 mM NaCl, 1 mM PMSF, 1 mM aprotinin, 10 μg/mL leupeptin, 50 mM Tris-Cl, pH 7.4). The cell lysate was cleared by centrifuging at 12,000 rpm for 25 min. Cell lysate containing 50 μg protein was separated by 10% sodium dodecyl sulfate polyacrylamide gel electrophoresis, and the protein was transferred onto polyvinylidene fluoride membrane. After blocking with 1% BSA, the polyvinylidene fluoride membrane was incubated with the primary antibodies (VEGF and actin) at 4 °C overnight, followed by incubation with appropriate secondary antibody for 1 h, and stained with enhanced chemiluminescence (ECL). The level of the targeted proteins was photographed and analyzed using a UVP gel analysis system (iBox Scientia 600; UVP, LLC., CA, USA).

ELISA to detect VEGF in vitro

The extracts of protamine NP/HAO CaAlg hydrogel were co-incubated with HUVECs (1×10^5 cells/well) seeded in 24-well plates for 24 h in an incubator set at 37 °C, 5% CO_2. The supernatants were collected and the amount of secreted VEGF was measured using VEGF enzyme-linked immunosorbent assay (ELISA) kit (R&D, USA) according to the kit instructions.

Evaluation of diabetic rat wound models

To evaluate the diabetic wound treatment with hydrogel dressings, streptozotocin (STZ; Sigma-Aldrich Co.) was injected into Sprague–Dawley (SD) rats intraperitoneally at a dosage of 100 mg/kg/body weight once per day for four consecutive days until the animals' blood glucose levels were > 300 mg/dL. This proved that a hyperglycemic phenotype was formed and that type 1 diabetes was induced in the SD rats. The performance of the protamine NPs/HAO CaAlg hydrogel as a wound dressing on type 1 diabetes in SD rats was evaluated. The rats were anesthetized with 3.5% chloral hydrate (via abdominal cavity injection), and full-thickness skin injures were obtained by cutting a circle, 2 cm in diameter, on the back skin. PBS, CaAlg hydrogel, and the protamine NP/HAO CaAlg hydrogel were separately placed on the surface of the wound twice daily for 2 weeks. To evaluate the antibacterial activities of protamine NPs/HAO CaAlg hydrogel in vivo, the bacteria from the wound site after application of the formulation was obtained by using the sterile cotton swab to extract the tissue exudate in the animal wound site on days 1, 3, 7, and 14 and were cultured with liquid nutrient broth medium. After shaking at 220 rpm/min for 3 h, the bacterial suspensions were plated on agar plates for 24 h and photographed by counting the number of viable bacterial cells. Wound areas were measured and photographed on days 1, 3, 7, and 14 with a sterile ruler placed beside the wound. On days 1, 3, 7, and 14, the muscle and skin around the wound were excised and fixed in 10% buffered formalin. The tissue was embedded in paraffin and sectioned vertically, and the sections were stained with hematoxylin and eosin (H&E) and examined by light microscopy. All animal studies were conducted according to the regulations for animal experimentation issued by the State Committee of Science and Technology of the People's Republic of China.

Results

Formation and characterization of protamine NPs/HAO CaAlg hydrogel

Protamine NPs were prepared by a desolvation method, as described previously [27]. The nanostructured investigation of synthesized protamine NPs was carried out using a transmission electron microscope (JEM-1200EX; JEOL, Tokyo, Japan) and dynamic light scattering (Zetasizer Nano ZS; Malvern Instruments, Malvern, UK) to decipher the geometry and particle size distribution. The obtained protamine NPs

were monodisperse and spherically shaped particles with varying diameters, which ranged from 43.8 to 190.1 nm (Fig. 2a, b). The average hydrodynamic diameter of the protamine NPs was 92.3 ± 14.3 nm and the polydispersity index was 0.019, indicating good monodispersity and uniformity. The mean zeta potential of the protamine NPs was +23.7 ± 2.5 mV (Fig. 2d), suggesting the positive surface polarity of protamine NPs. SEM analysis of protamine NP/HAO CaAlg hydrogel revealed that the hydrogel appeared to have high surface roughness with a uniform and porous morphology, indicating the possibility of loading NPs and HAO into smaller pores in the hydrogel (Fig. 2c). It was also found that the CaAlg hydrogel showed the higher encapsulation efficiency of HAO at 85.4% ± 6.2%. The loading rate of HAO in CaAlg hydrogel was 5.4 ± 1.1%.

Rheological properties, swelling ratio, and drug release of protamine NP/HAO CaAlg hydrogel in vitro

Figure 3a illustrates that CaAlg hydrogel and protamine NP/HAO CaAlg hydrogel showed greater elastic properties and that the elastic (storage) modulus (G′) was greater than the viscous (loss) modulus (G″) in both gels. In addition, the phase angle (δ) in both gel systems did not show an obvious variation at the frequency range of Hz, and these were valued at around 10^0. The thermal stability of the gels was determined by detecting the change of the complex modulus (G*) and complex viscosity (η*) from 25 to 45 °C at constant frequency and shear. Figure 3b indicates that at the tested temperature, both gels were very stable, and their complex modulus (G*) and complex viscosity (η*) had not changed much. The addition of the NPs and drug did not affect the microstructure of the gel system and both gels showed similar rheological behavior.

In terms of evaluating the gels for swelling capacity, the results (Fig. 3c) showed that the protamine NP/HAO CaAlg hydrogel tended to absorb more water and their swelling ratios were increased in association with medium pH enhancement. This indicated that in a medium with a pH of 3.0, which was below the pKa value of CaAlg that ranged from 3.2 to 4.0, most of the carboxylic acid groups in the CaAlg hydrogel were in the form of –COOH, thus leading to a polymer–polymer combination owing to the hydrogen bond between –COOH, instead of a hydrogen bond between –COOH and water. Therefore, the CaAlg hydrogel had shrunk and was difficult to swell. When the CaAlg hydrogel was immersed in PBS solution at pH levels of 6.0 and 8.0, the carboxylic acid groups were ionized and predominantly in the form of $–COO^-$. The electrostatic repulsion between $–COO^-$ groups resulted in swelling of the hydrogel. At the same time, the hydrogen bonds between $–COO^-$ and H_2O were easily formed; therefore, the hydrogel was significantly swollen in the simulated diabetic wound fluid medium at a pH level of 8.0.

In terms of the drug-release process from NPs, the protamine NPs/HAO CaAlg hydrogel showed different release

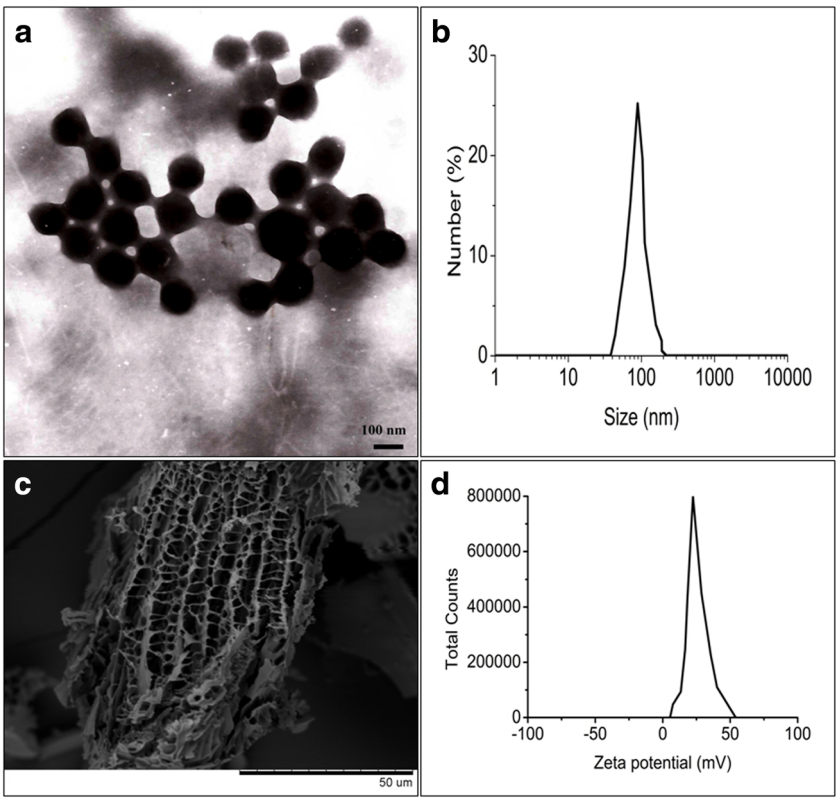

Fig. 2 Schematic representation of protaimine NPs/HAO CaAlg hydrogel. **a** TEM image of protamine NPs. **b** DLS analysis of the obtained protamine NPs. **c** SEM image of protamine NPs/HAO CaAlg hydrogel. **d** Zeta potential distribution of protamine NPs

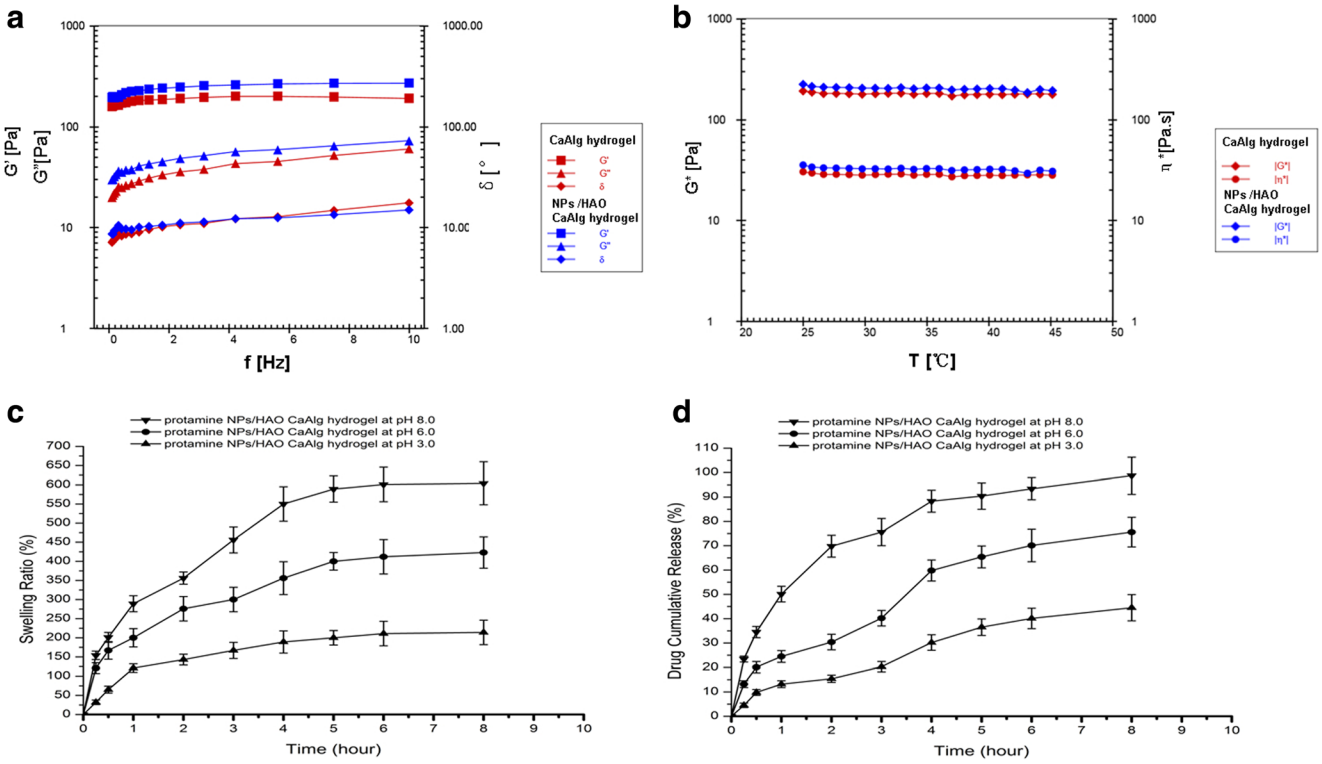

Fig. 3 Determination of the elastic (storage) modulus (G′) and viscous (loss) modulus (G″) (**a**), the complex modulus (G*) and complex viscosity (η*) (**b**) of protaimine NPs/HAO CaAlg hydrogel. **c** Swelling variation of protaimine NPs/HAO CaAlg hydrogel under different pH condition. **d** pH-responsive drug delivery of HAO from protaimine NPs/HAO CaAlg hydrogel for a period of 8 h under different pH condition

patterns in the medium with different pH levels. In the medium with a pH level of 3.0, which mimicked the acidic microenvironment, the protonation of the ionized $–COO^-$ groups led to the shrinkage of CaAlg hydrogel and blocked the release of the drug from the hydrogel. The hydrogel showed a slower drug-release pattern in vitro and about 44.5% of total HAO were released within 8 h. In the stimulated diabetic wound medium at a pH level of 8.0, CaAlg hydrogel was swollen by absorbing more water, leading to the disruption and looseness of the gelling structure of CaAlg, further facilitating the fast release of NPs and HAO. There was a faster accumulative release process in the protamine NP/HAO CaAlg hydrogel, where 98.7% of the total HAO were released from the hydrogel within 8 h. The drug release from the CaAlg hydrogel at a pH level of 8.0 was about 2.2-fold faster than that at a pH level of 3.0. These results indicated that the increased drug release at pH 8.0 could be attributed to the pH-dependent activity of the CaAlg hydrogel. The mechanism involved in greater drug release at pH 8.0 could be due to the increase in the absorption of CaAlg hydrogel under mildly alkaline conditions, thus facilitating the faster release of protamine NPs and HAO from the CaAlg hydrogel. Herein, the in vitro release profile of drugs from the pH-sensitive CaAlg hydrogel presented a pH-dependent pattern, and drug-release rates gradually increased at basic pH levels and delayed at acidic pH levels. This further confirmed that the protamine NP/HAO CaAlg hydrogel assessed specific and effective drug delivery to the alkaline diabetic wound site.

MTT assay and hemolysis analysis

The MTT results (Fig. 4a) showed that when HFF cells and HUVECs were treated with extracts of the protamine NP/HAO-loaded CaAlg hydrogel ranging from 10 to 100 μg/mL for 24 h, no obvious cytotoxic activities or cell proliferation promotion were observed in both cells. The results (Fig. 4b) also showed that when red blood cells were treated with extracts of the protamine NP/HAO CaAlg hydrogel at 100 μg/mL, and the serum or plasma appeared transparent and colorless. This proved that the hemolysis effect induced by the hydrogel was very low and the protamine NP/HAO CaAlg hydrogel exhibited good biocompatibility and safety at the test dose, under our experimental conditions.

Antibacterial effect of protamine NPs/HAO CaAlg hydrogel

The antibacterial activity of protamine NPs/HAO CaAlg hydrogel was evaluated against Gram-positive strains viz. *S. aureus* and Gram-negative strains viz. *E. coli*. It was evident

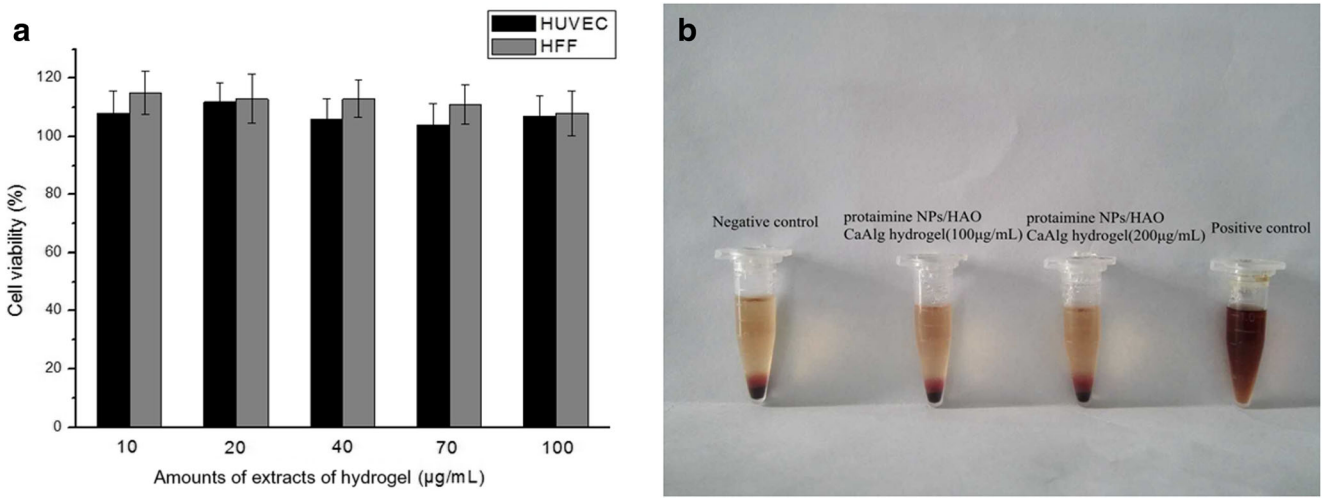

Fig. 4 Results of cell viability assay and hemolysis assay **a** viability of HFF cells and HUVECs after incubating with different amounts of extracts of protaimine NPs/HAO CaAlg hydrogel for 24 h ($n = 3$). **b** Hemolysis determined by observing the color change of the serum and plasma after 24-h incubation with extracts of protaimine NPs/HAO CaAlg hydrogel, respectively

in Fig. 5a, b that the blank CaAlg hydrogel showed no obvious antibacterial activity against Gram-negative bacteria and Gram-positive bacteria. With the addition of positively charged protamine NPs, the protamine NPs/HAO CaAlg hydrogel significantly enhanced the inhibition of the growth of *E. coli* and *S. aureus* with increasing concentration of protamine NPs. The minimum bactericidal concentrations (MBCs) of protamine NPs loaded in the CaAlg hydrogel were 40 μg/mL against *E. coli* and 60 μg/mL against *S. aureus*. These results suggested that as the protamine NPs had positive charges, protamine NPs/HAO CaAlg hydrogel adhered to the negative charged surface of *E. coli* and *S. aureus* cells with a high probability. A strong interaction with both Gram-positive and Gram-negative bacteria by electro-static interaction might be a key reason that explains the effective antibacterial activity of protamine NPs/HAO CaAlg hydrogel. Compared with the Gram-positive bacterium, Gram-negative bacteria with a comparatively higher negative surface charge was easily combined with protamine NPs/HAO CaAlg hydrogel, thus resulting in more effective killing. In addition, the protamine NPs/HAO CaAlg hydrogel group also exhibited an increased release of bacterial DNA and RNA, suggesting that the protamine NPs/HAO CaAlg hydrogel disrupted the cell wall and increased membrane permeability, thus facilitating the fast release of bacterial DNA and RNA. Severe cell wall damage was observed by scanning electron microscopy (Fig. 5d), insofar as the bacteria lost their cocci or rod shape, and lots of pits and cavities appeared at the cell surface. The protamine NP/HAO CaAlg hydrogel tended to adhere to the cell surface and disrupt the cell membrane's integrity, thus leading to an outburst of cell materials.

Angiogenesis of protaimine NPs/HAO CaAlg hydrogel in viro

Tubule formation was a key step in the angiogenic process. The results (Fig. 6b, d) showed that when compared with the control group and protamine NP CaAlg hydrogel, the protamine NP/HAO CaAlg hydrogel enhanced endothelial cell capillary-like loop formation, as assessed by quantification of the loop number on HUVECs with the mediation of HAO in a dose-dependent pattern. Moreover, as shown in Fig. 6a, c, we also observed a significant increase in the number of migrating HUVECs upon the mediation of HAO. At the same time, as shown in Fig. 6e, VEGF expression levels were obviously increased following treatment with the addition of HAO, while no increase was found in HUVECs without HAO treatment. To further confirm enhanced VEGF production induced by protamine NP/HAO CaAlg hydrogel, the expression of VEGF in HUVECs was evaluated by ELISA and VEGF secretion efficiency was determined by calculating the ratio of VEGF production from HUVEC treated with the extract of the protamine NP/HAO-loaded CaAlg hydrogel to that from the untreated cells as control to provide baseline level of VEGF production (%). As seen in Fig. 6f, compared with the control group and protamine NP CaAlg hydrogel, addition of HAO exhibited the higher VEGF secretion efficiency, while there was no obvious variation on VEGF secretion between the control group and protamine NP-loaded CaAlg hydrogel-treated group. Taken together, this suggested that HAO may induce angiogenesis by stimulating the proliferation of vascular endothelial cells and promoting the expression of VEGF, indicating that the protamine NP/HAO CaAlg hydrogel may promote angiogenesis through HAO induced the stimulation of VEGF.

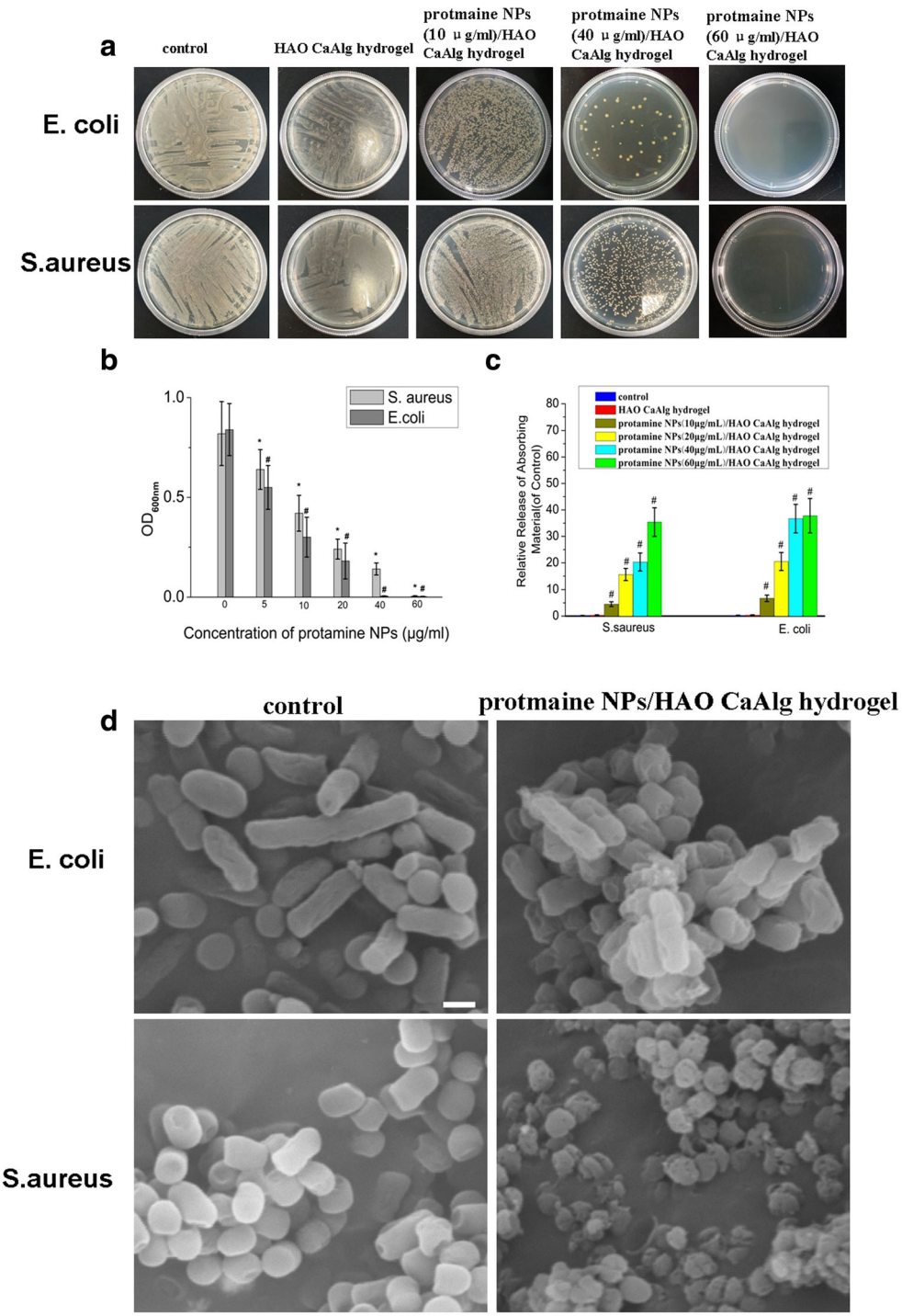

Fig. 5 Assessment of antibacterial activity of protaimine NPs/HAO CaAlg hydrogel against Gram-positive strains viz. *S. saureus* and Gram negative strains viz. *E. coli*. **a** Photographs of culture plates of *E. coli* and *S. aureus* after exposure to protaimine NPs/HAO CaAlg hydrogel with containing different concentration of NPs. **b** $OD_{600\ nm}$ of bacterial suspension treated with protaimine NPs/HAO CaAlg hydrogel. These data represented three separate experiments and were presented as the mean values ± SD. $^{*}P < 0.05$ versus $OD_{600\ nm}$ of *S. aureus* treated with control group, $^{\#}P < 0.05$ versus $OD_{600\ nm}$ of *E. coli* treated with control group. **c** Relative release of 260 nm absorbing materials from protaimine NPs/HAO CaAlg hydrogel treated *E. coli* and *S. aureus*. These data represented three separate experiments and were presented as the mean values ± SD. $^{\#}P < 0.05$ versus control group. **d** SEM images of bacteria treated with protaimine NPs/HAO CaAlg hydrogel

Assessment of the antibacterial activity of protaimine NPs/HAO CaAlg hydrogel and wound closure analysis

From Fig. 7a, it appears that the protamine NP/HAO CaAlg hydrogel formed an insulating layer that protected the diabetic wound site from being infected by bacteria. In addition, protamine NPs laden with CaAlg hydrogel showed enhanced antibacterial properties and they protected wounds from infection. Figure 7b illustrates that there was significant bacterial proliferation observed in both PBS-treated and blank hydrogel-treated diabetic wound sites with severe ulceration and festering within 3 days. Both PBS-treated and blank hydrogel-treated diabetic wounds became infected within 3 days and showed severe inflammation with a wound closure rate of 54.9% for PBS and 59.8% for CaAlg hydrogel within 5 days. In contrast, when covered with protamine NP/HAO-

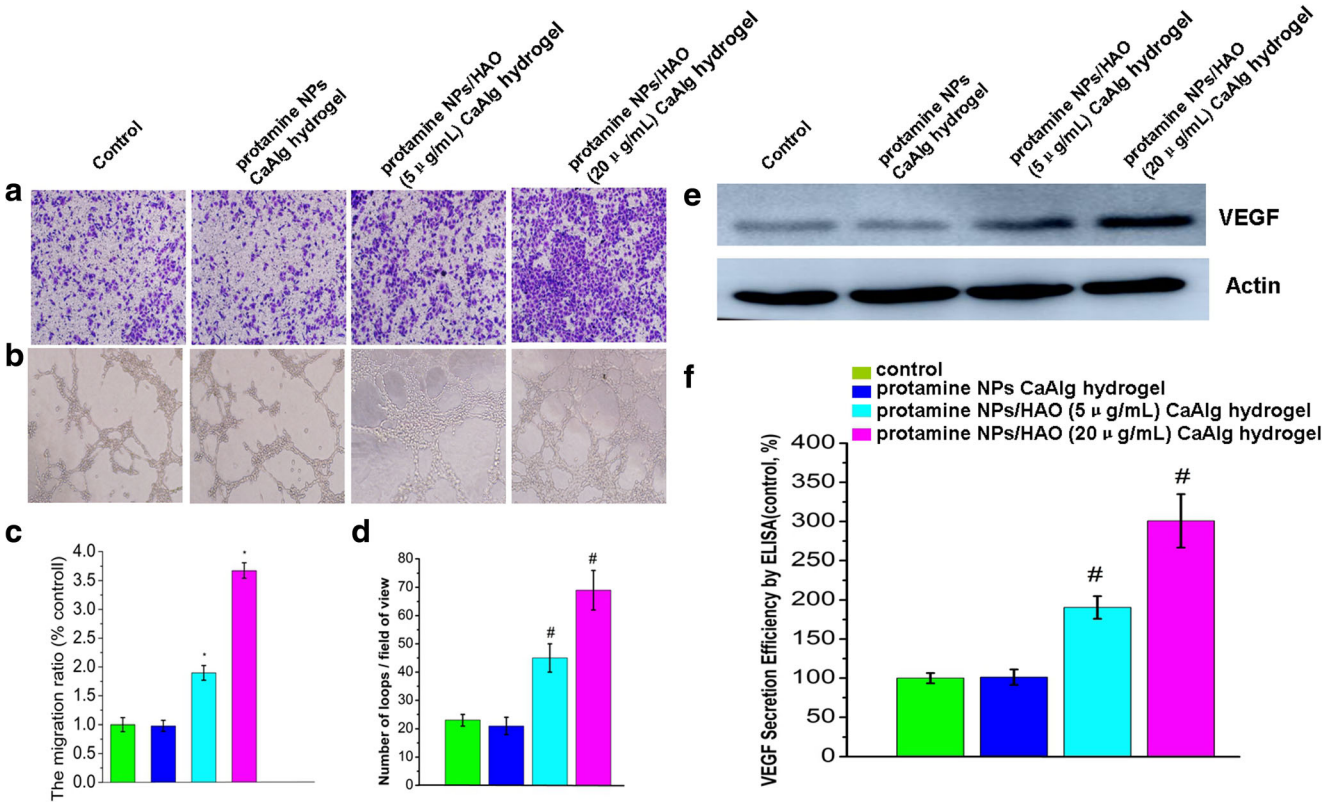

Fig. 6 Protaimine NPs/HAO CaAlg hydrogel enhanced HUVECs capillary-like tube formation and migration. **a** Migration of HUVECs treated with different kinds of CaAlg hydrogel assessed by transwell assay and **c** migration ratios were measured and compared with control. Data represented the mean ± SD ($n = 3$), $^{*}P < 0.05$ versus control group. **b** Representative images of HUVEC capillary morphogenesis after treated with different kinds of CaAlg hydrogel for 24 h, and **d** the numbers of loops were measured and compared with control. Data represented the mean ± SD ($n = 3$), $^{\#}P < 0.05$ versus control group. **e** Western blot analyses of the expression levels of VEGF when HUVEC were treated with different kinds of CaAlg hydrogel. **f** VEGF secretion treated with different kinds of CaAlg hydrogel by ELISA on HUVECs. Data represented the mean ± SD ($n = 3$), $^{\#}P < 0.05$ versus control group

loaded CaAlg hydrogel, the wound did not show obvious ulceration, nor did it fester, and the bacterial proliferation was completely inhibited. Moreover, the hydrogel showed excellent adherence to the wound tissue and the wound fluid was sufficiently absorbed by the hydrogels. Wounds treated with the protamine NP/HAO CaAlg hydrogel showed calluses and slight inflammation, with signs of better and faster healing within 3 days; moreover, the rate of wound closure was about 73.5% within 5 days. Within 14 days, the wound closure rate increased to 96.8%. Similarly, after being treated with PBS and CaAlg hydrogel, the rates of wound closure were lower and valued at 88.8% and 88.5% within 14 days, respectively.

Histological observations in the wound area

Histological observations (Fig. 8) revealed that within 7 days of treatment, there were fewer inflammatory cells and neutrophils observed at the wound site treated with protamine NPs/HAO CaAlg hydrogel when compared with the control group and blank CaAlg hydrogel. This indicated that as the protamine NPs/HAO CaAlg hydrogel significantly inhibited antibacterial growth, the diabetic wound site was protected from infection and acute local inflammation was further reduced, thus accelerating wound repair. Furthermore, at the initial 3 days of treatment, the addition of HAO strengthened blood perfusion to the wound, and the granulation tissue in the wound bed was filled with fewer inflammatory cell infiltrates and more congested blood vessels, indicating that HAO induced marked endothelial cell proliferation and neoangiogenesis when compared to the other groups. On the seventh day, when compared with the control and CaAlg hydrogel, the granulation tissues at the diabetic wound site treated with protamine NPs/HAO CaAlg hydrogel contained comparatively fewer inflammatory cells, as well as more collagen and fibroblasts; fewer blood-proliferating capillaries were also observed. This suggests that the protamine NPs/HAO CaAlg hydrogel significantly expedited complete regeneration of the epidermis and dermis. After 14 days, diabetic wounds covered with the protamine NPs/HAO CaAlg hydrogel showed a regenerated dermis and

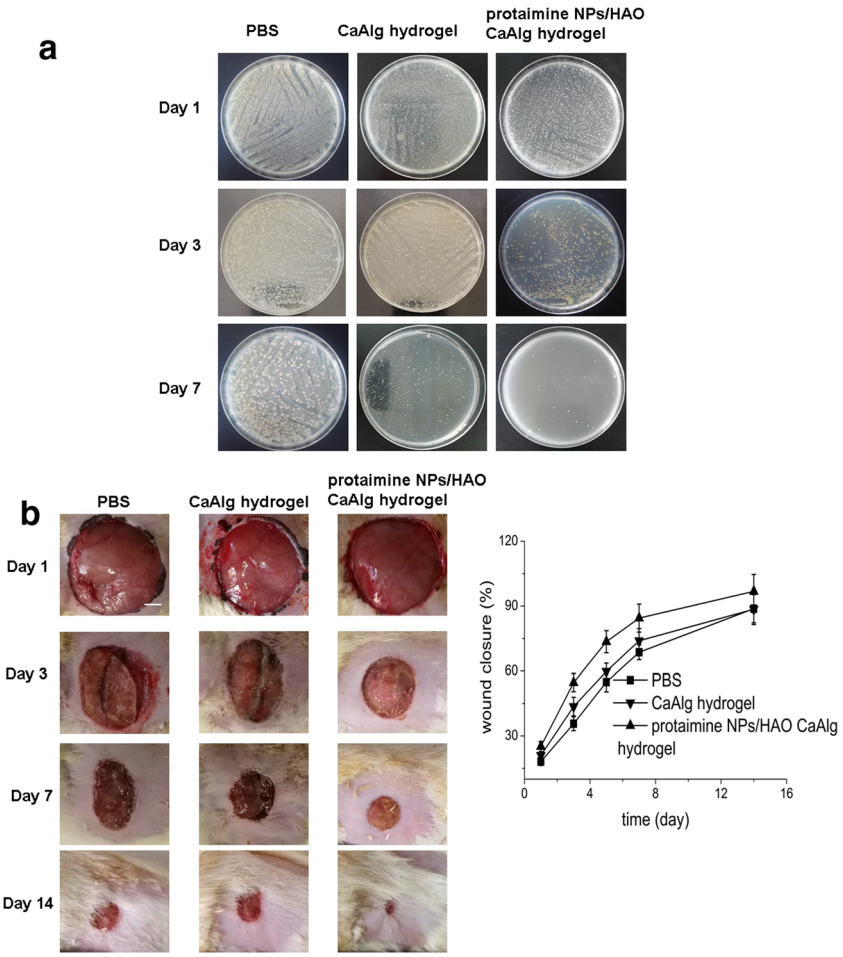

Fig. 7 Assessment of antibacterial activity of hydrogel and wound closure analysis. **a** Photographs of culture plates of bacteria from the diabetic wound when treated with PBS, CaAlg hydrogel and protaimine NPs/HAO-loaded CaAlg hydrogel. **b** Assessment of wound closure of the diabetic wounds on days 1, 3, 7, and 14 postoperation under the treatment of PBS and different CaAlg hydrogels.

epithelium. It was proven that protamine NsP/HAO CaAlg hydrogel contributed to a faster wound-healing process, likely due to the anti-inflammatory and antimicrobial activity of protamine NPs, and HAO also contributed to angiogenesis promotion.

Discussion

The inflammatory phase is a crucial step in diabetic wound healing that is frequently stalled; this promotes a pro-inflammatory status that contributes to the development of chronic, non-healing, diabetic ulcers [32]. Chronic wounds are colonized by diverse bacterial microflora, and bacteria residing within the wound bed is capable of directly or indirectly perpetuating inflammation and impaired healing responses [33–36]. It was supposed that local inflammation damaged the blood vessels and prolonged angiogenesis, thus inhibiting the wound-healing effects in the early phase of the wound-healing process [37]. In this study, the anti-infective and wound-healing abilities of protamine NPs/HAO CaAlg hydrogel was evaluated by constructing a wound-healing model of type 1 diabetes in SD rats. It was found that compared with CaAlg hydrogel, protamine NPs/HAO CaAlg hydrogel demonstrated stronger bactericidal behavior and accelerated wound-healing process by promoting angiogenesis. The results suggested that CaAlg hydrogel showed no obvious antibacterial activity against Gram-negative bacteria and Gram-positive bacteria. With the addition of positively charged protamine NPs, the protamine NP/HAO CaAlg hydrogel significantly enhanced the inhibition of the growth of *E. coli* and *S. aureus*. Furthermore, transwell, capillary-like tube formation and ELISA results also confirmed that compared with cells treated with CaAlg hydrogel, protamine NPs/HAO CaAlg hydrogel enhanced cell migration, endothelial cell capillary-like loop formation and the secretion of VEGF. In vivo, the protamine NPs/HAO CaAlg hydrogel displayed the best anti-inflammatory effects by significantly enhancing the inhibition bacterial growth. Furthermore, it may also promote the formation of blood vessel at the wound site and accelerate wound contraction and healing. The protamine NPs/HAO CaAlg hydrogel absorbed more wound exudates, which maintained the wound's moist microenvironment and facilitated the removal of foreign substances. In addition, the

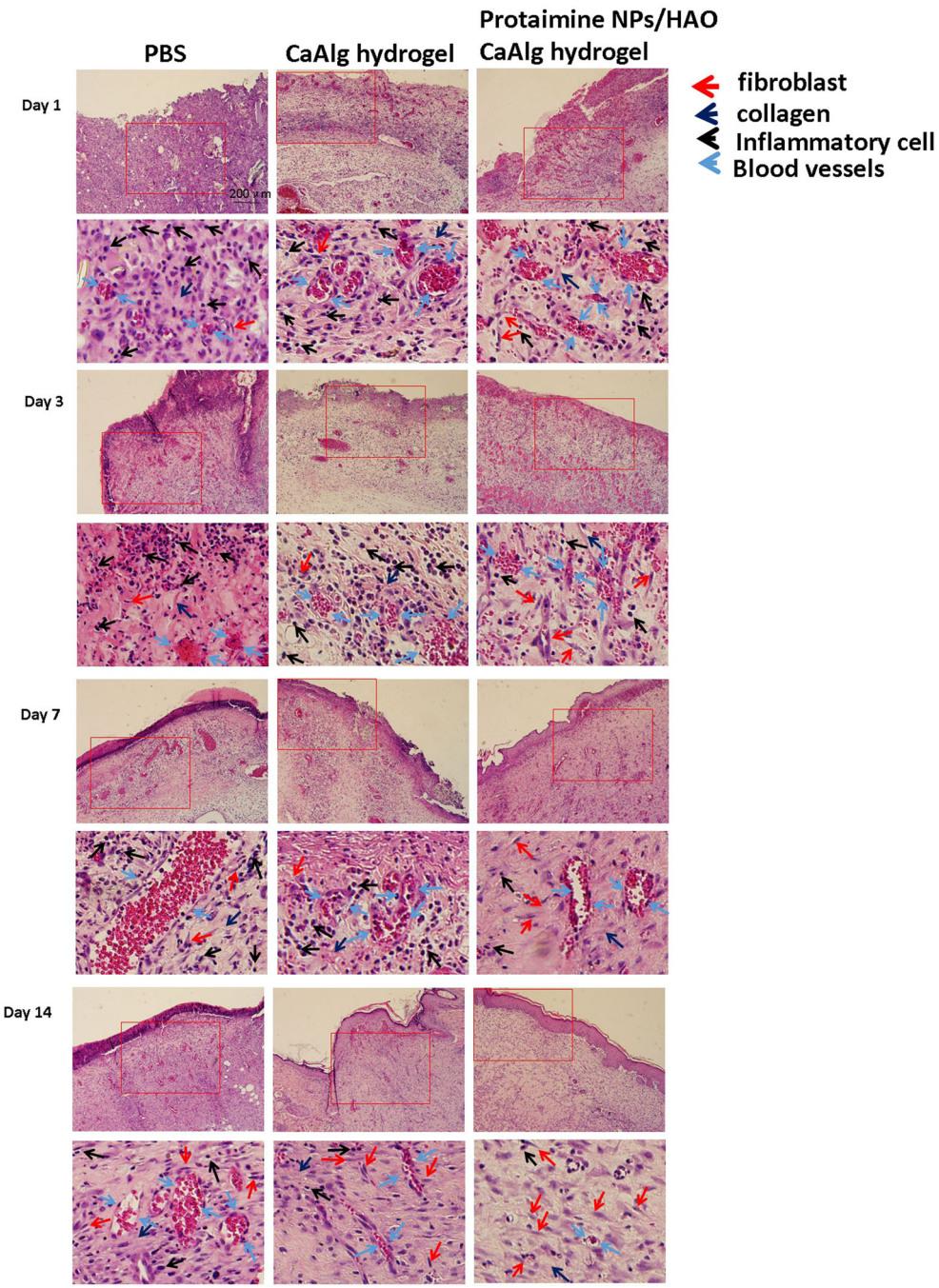

Fig. 8 H&E staining of tissue sections treated with PBS, CaAlg hydrogel, and protaimine NPs/HAO CaAlg hydrogel on days 1, 3, 7, and 14

hydrogel controlled the more rapid and complete drug release in the medium at pH 8.0, which mimicked the diabetic wound microenvironment, thus facilitating the faster release of protamine NPs and HAO to enhance their anti-bacterial activity and angiogenesis effects. A histological investigation was performed on days 1, 3, 7, and 14, respectively. The results showed that on day 3, many inflammatory cells were found and infiltrated into the wound site treated with PBS and the CaAlg hydrogel. This indicated that the acute local inflammation was induced. On the other hand, owing to the enhanced antibacterial properties of protamine NPs, the wound site treated with the protamine NPs/HAO CaAlg hydrogel did not exhibit an acute inflammatory reaction and fewer amounts of neutrophils and inflammatory cells were observed. Furthermore, with the fast distribution of HAO from the hydrogel at the diabetic wound site, the strongest blood perfusion was induced following significant formation of fibroblasts, granulation tissues, and blood vessels at the wound site. With the acceleration of wound healing and re-epithelialization, local inflammation was further reduced and the blood perfusion in the annular blood supply area was gradually weakened. The histological examination also confirmed that

when compared with the control and CaAlg hydrogel, the protamine NPs/HAO CaAlg hydrogel promoted re-epithelialization, as represented by the formation of more fibroblast and collagen. Taken together, the protamine NPs/HAO CaAlg hydrogel contributed to the rapid healing of diabetic skin wound by reducing chronic inflammation and promoting granulation tissue formation, angiogenesis, wound contraction, and re-epithelialization.

Conclusion

In summary, a pH-responsive CaAlg hydrogel laden with protamine NPs and HAO was successfully prepared and exhibited good homogeneity, biocompatibility, and pH-responsive drug release. The results demonstrated that the protamine NPs/HAO CaAlg hydrogel showed a significant inhibitory effect on Gram-positive and Gram-negative bacteria with the mediation of anti-bacterial protamine NPs, thus reducing bacteria-induced chronic inflammation at the wound site and promoting wound-healing effects. The addition of HAO also enhanced HUVEC migration, capillary-like tube formation and the secretion of VEGF in vitro. Furthermore, it may also promote the formation of blood vessel at the wound site and accelerate wound healing. These results showed that the obtained hydrogel containing protamine NPs and HAO contributed to the rapid healing of diabetic skin wounds, possibly rendering it a promising therapeutic strategy for the management of diabetic ulcers.

Acknowledgements English-language editing of this manuscript was provided by Journal Prep.

Compliance with ethical standards

All animal studies were conducted according to the regulations for animal experimentation issued by the State Committee of Science and Technology of the People's Republic of China.

Conflict of interest The authors declare that they have no conflicts of interest.

References

1. Shaw JE, Sicree RA, Zimmet PZ. Global estimates of the prevalence of diabetes for 2010 and 2030. Diabetes Res Clin Pract. 2010;87(1):4–14.
2. Wang X, Sng MK, Foo S, Chong HC, Lee WL, Tang MBY, et al. Early controlled release of peroxisome proliferator-activated Receptorbeta/delta agonist GW501516 improves diabetic wound healing through redox modulation of wound microenvironment. J Control Release. 2015;197:138–47.
3. Gao M, Nguyen TT, Suckow MA, Wolter WR, Gooyit M, Mobashery S, et al. Acceleration of diabetic wound healing using a novel protease-anti-protease combination therapy. Proc Natl Acad Sci U S A. 2015;112(49):15226–31.
4. Erba P, Ogawa R, Ackermann M, Adini A, Miele LF, Dastouri P, et al. Angiogenesis in wounds treated by microdeformational wound therapy. Ann Surg. 2011;253(2):402–9.
5. Greene AK, Puder M, Roy R, Arsenault D, Kwei S, Moses MA, et al. Microdeformational wound therapy: effects on angiogenesis and matrix metalloproteinases in chronic wounds of 3 debilitated patients. Ann Plast Surg. 2006;56(4):418–22.
6. Peng C, Chen B, Kao HK, Murphy G, Orgill DP, Guo L. Lack of fgf-7 further delays cutaneous wound healing in diabetic mice. Plast Reconstr Surg. 2011;128(6):673e–84e.
7. Kirketerp-Møller K, Jensen PØ, Fazli M, et al. Distribution, organization, and ecology of bacteria in chronic wounds. J Clin Microbiol. 2008;46(8):2717–22.
8. McArdle C, Lagan KM, McDowell DA. The pH of wound fluid in diabetic foot ulcers—the way forward in detecting clinical infection? Curr Diabetes Rev. 2014;10(3):177–81.
9. Schneider LA, Korber A, Grabbe S, Dissemond J. Influence of pH on wound-healing: a new perspective for wound-therapy? Arch Dermatol Res. 2007;298(9):413–20.
10. Chen H, Xing X, Tan H, Jia Y, Zhou T, Chen Y, et al. Covalently antibacterial alginate-chitosan hydrogel dressing integrated gelatin microspheres containing tetracycline hydrochloride for wound healing. Mater Sci Eng C Mater Biol Appl. 2017;70(Pt 1):287–95.
11. Chopra P, Nayak D, Nanda A, Ashe S, Rauta PR, Nayak B. Fabrication of poly(vinyl alcohol)-carrageenan scaffolds for cryopreservation: effect of composition on cell viability. Carbohydr Polym. 2016;147:509–16.
12. Park SY, Lee HU, Lee YC, Kim GH, Park EC, Han SH, et al. Wound healing potential of antibacterial microneedles loaded with green tea extracts. Mater Sci Eng C Mater Biol Appl. 2014;42:757–62.
13. Napavichayanun S, Amornsudthiwat P, Pienpinijtham P, Aramwit P. Interaction and effectiveness of antimicrobials along with healing-promoting agents in a novel biocellulose wound dressing. Mater Sci Eng C Mater Biol Appl. 2015;55:95–104.
14. Li JF, Fu XB, Sheng ZY, Sun TZ. Redistribution of epidermal stem cells in wound edge in the process of re-epithelialization. Zhonghua Yi Xue Za Zhi. 2003;83(3):228–31.
15. Icli B, Nabzdyk CS, Lujan-Hernandez J, Cahill M, Auster ME, Wara AKM, et al. Regulation of impaired angiogenesis in diabetic dermal wound healing by microRNA-26a. J Mol Cell Cardiol. 2016;91:151–9.
16. Xu J, Zgheib C, Hu J, Wu W, Zhang L, Liechty KW. The role of microRNA-15b in the impaired angiogenesis in diabetic wounds. Wound Repair Regen. 2014;22(5):671–7.
17. Lim YC, Bhatt MP, Kwon MH, Park D, Na SH, Kim YM, et al. Proinsulin C-peptide prevents impaired wound healing by activating angiogenesis in diabetes. J Invest Dermatol. 2015;135(1):269–78.
18. Zhou K, Ma Y, Brogan MS. Chronic and non-healing wounds: the story of vascular endothelial growth factor. Med Hypotheses. 2015;85(4):399–404.
19. West DC, Hampson IN, Arnold F, Kumar S. Angiogenesis induced by degradation products of hyaluronic acid. Science. 1985;228(4705):1324–6.
20. West DC, Kumar S. The effect of hyaluronate and its oligosaccharides on endothelial cell proliferation and monolayer integrity. Exp Cell Res. 1989;183(1):179–96.
21. Sattar A, Rooney P, Kumar S, Pye D, West DC, Scott I, et al. Application of angiogenic oligosaccharides of hyaluronan increases blood vessel numbers in rat skin. J Invest Dermatol. 1994;103(4):576–9.

22. Montesano R, Kumar S, Orci L, Pepper MS. Synergistic effect of hyaluronan oligosaccharides and vascular endothelial growth factor on angiogenesis in vitro. Lab Investig. 1996;75(2):249–62.
23. Xu Q, A S, Gao Y, Guo L, Creagh-Flynn J, Zhou D, et al. A hybrid injectable hydrogel from hyperbranched PEG macromer as a stem cell delivery and retention platform for diabetic wound healing. Acta Biomater. 2018;75:63–74.
24. Xu Q, Guo L, A S, Gao Y, Zhou D, Greiser U, et al. Injectable hyperbranched poly(β-amino ester) hydrogels with on-demand degradation profile to match wound healing process. Chem Sci. 2018;9(8):2179–87.
25. Pustam A, Smith C, Deering C, Grosicki KMT, Leng TY, Lin S, et al. Interactions of protamine with the marine bacterium, Pseudoalteromonas sp. NCIMB 2021. Lett Appl Microbiol. 2014;58(3):225–30.
26. Johansen C, Verheul A, Gram L, Gill T, Abee T. Protamine-induced permeabilization of cell envelopes of gram-positive and gram-negative bacteria. Appl Environ Microbiol. 1997;63(3):1155–9.
27. Liu M, Feng B, Shi Y, Su C, Song H, Cheng W, et al. Protamine nanoparticles for improving shRNA-mediated anti-cancer effects. Nanoscale Res Lett. 2015;10:134.
28. Shen Y, Zhao L, Su C, Shi Y, Yang G, Liu X. Efficient nucleus-targeted delivery of gene by nuclear localization signal peptides-mediated nanoparticles. J Biomater Tissue Eng. 2016;6(11):924–30.
29. Wang T, Zheng Y, Shen Y, et al. Chitosan nanoparticles loaded hydrogels promote skin wound healing through the modulation of reactive oxygen species. Artif Cells Nanomed Biotechnol 2017:1–12.
30. Zhao L, Su R, Cui W, Shi Y, Liu L, Su C. Preparation of biocompatible heat-labile enterotoxin subunit B-bovine serum albumin nanoparticles for improving tumor-targeted drug delivery via heat-labile enterotoxin subunit B mediation. Int J Nanomedicine. 2014;9:2149–56.
31. Wang Q, Shi Y, Yang G, Zhao L. Sodium alginate coated chitosan nanoparticles enhance antitumor efficiency via smartly regulating drug release at different pH. J Biomater Tissue Eng. 2017;7(2):127–33.
32. Moura LI, Dias AM, Suesca E, et al. Neurotensin-loaded collagen dressings reduce inflammation and improve wound healing in diabetic mice. Biochim Biophys Acta. 2014;1842(1):32–43.
33. Park S, Rich J, Hanses F, Lee JC. Defects in innate immunity predispose C57BL/6J-Leprdb/Leprdb mice to infection by Staphylococcus aureus. Infect Immun. 2009;77(3):1008–14.
34. Schierle CF, De la Garza M, Mustoe TA, Galiano RD. Staphylococcal biofilms impair wound healing by delaying reepithelialization in a murine cutaneous wound model. Wound Repair Regen. 2009;17(3):354–9.
35. Siddiqui AR, Bernstein JM. Chronic wound infection: facts and controversies. Clin Dermatol. 2010;28(5):519–26.
36. Fazli M, Bjarnsholt T, Kirketerp-Møller K, Jørgensen A, Andersen CB, Givskov M, et al. Quantitative analysis of the cellular inflammatory response against biofilm bacteria in chronic wounds. Wound Repair Regen. 2011;19(3):387–91.
37. Hansen SL, Myers CA, Charboneau A, Young DM, Boudreau N. HoxD3 accelerates wound healing in diabetic mice. Am J Pathol. 2003;163(6):2421–31.